Post-buckling analysis of Timoshenko beams with temperature-dependent physical properties under uniform thermal loading

Şeref Doğuşcan Akbaş* and Turgut Kocatürk[a]

Department of Civil Engineering, Yıldız Technical University, Davutpasa Campus, 34210 Esenler, Istanbul, Turkey

Abstract. Post-buckling behavior of Timoshenko beams subjected to uniform temperature rising with temperature dependent physical properties are studied in this paper by using the total Lagrangian Timoshenko beam element approximation. The beam is clamped at both ends. In the case of beams with immovable ends, temperature rise causes compressible forces end therefore buckling and post-buckling phenomena occurs. It is known that post-buckling problems are geometrically nonlinear problems. Also, the material properties (Young's modulus, coefficient of thermal expansion, yield stress) are temperature dependent: That is the coefficients of the governing equations are not constant in this study. This situation suggests the physical nonlinearity of the problem. Hence, the considered problem is both geometrically and physically nonlinear. The considered highly non-linear problem is solved considering full geometric non-linearity by using incremental displacement-based finite element method in conjunction with Newton-Raphson iteration method. The beams considered in numerical examples are made of Austenitic Stainless Steel (316). The convergence studies are made. In this study, the difference between temperature dependent and independent physical properties are investigated in detail in post-buckling case. The relationships between deflections, thermal post-buckling configuration, critical buckling temperature, maximum stresses of the beams and temperature rising are illustrated in detail in post-buckling case.

Keywords: temperature dependent physical properties; thermal post-buckling analysis; total lagrangian finite element model; Timoshenko beam; uniform temperature rise

1. Introduction

Nuclear power plants, Aerospace vehicles, thermal power plants etc. are subject to large thermal loadings. The design of structural elements (beams, plates, shells etc.) in the high thermal environments is very important in engineering applications. Especially, in the case of structural elements with immovable ends, temperature rise causes compressible forces end therefore buckling and post-buckling phenomena occurs. Understanding the buckling and post-buckling mechanism of structural elements is very important. It is known that buckling and post-buckling problems are nonlinear problems. In recent years, with the development of technology in aerospace engineering,

*Corresponding author, Ph.D. Student, E-mail: serefda@yahoo.com
[a]Professor, E-mail: kocaturk@yildiz.edu.tr

structural enginering, robotics and manufacturing make it inevitable to excessively use non-linear models that must be solved numerically. Because, closed-form solutions of large-deflection problems of beams with general loading and boundary conditions using elliptic integrals are limited. There have been a lot of studies on buckling and post-buckling of beams. Rao and Raju (1984) investigated thermal postbuckling of columns. Global descriptions of the properties of buckled states of nonlinearly thermoelastic beams and plates when heated at their ends and edges is investigated by Gauss and Antman (1984). Jekot (1996) investigated the thermal postbuckling of a beam made of physically nonlinear thermoelastic material by using the geometric equations in the von-Karman strain-displacement approximation. Li (2000) examined Thermal Post-Buckling of Rods with Pinned-Fixed Ends using the shooting method. Coffin and Bloom (1999) gave an elliptic integral solution for the symmetric post-buckling response of a linear elastic and hygrothermal beam with the two ends pinned. On the basis of exact nonlinear geometric theory of extensible beam and by using a shooting method, computational analysis for thermal post buckling behavior of beams with pinned-pinned, fixed-fixed and pinned-fixed ends were presented by Li and Cheng (2000), Li *et al.* (2002), Li and Zhou (2001). Thermal post-buckling responses of an elastic beam, with immovably simply supported ends and subjected to a transversely non-uniformly distributed temperature rising, were investigated by Li *et al.* (2003). Thermal post-buckling response of an immovably pinned-fixed Timoshenko beam subjected to a static transversely nonuniform temperature rise is numerically analyzed by using a shooting method by Li and Zhou (2003). Based on the finite element method, the analysis of heat conduction and structural stress and buckling are considered at the same time in the design optimization procedure by Chen *et al.* (2003). Vaz and Solano (2003, 2004) investigated thermal post-buckling of rods and came up with a closed form solution via uncoupled elliptical integrals. Large thermal deflections for Timoshenko beams subjected to transversely non-uniform temperature rise and with pinned-pinned as well as fixed-fixed ends are numerically analyzed by Li and Song (2006). Aristizabal-Ochao (2007) developed a new set of slope deflection equations for Timoshenko beam-columns which includes the combined effects of shear and bending deformations, and second-order axial load effects in a classical manner and emphasized the great importance of shear effects on static, tension and compression stability and dynamic behavior of elastomeric bearings used for seismic isolation. Both thermal buckling and post-buckling of pinned-fixed beams resting on an elastic foundation are investigated by Song and Li (2007). Vaz *et al.* (2007) examined a perturbation solution for the initial post-buckling of beams resting on elastic foundation and subjected to uniform thermal load. Parente and de Sousa (2008) investigated a simple and efficient methodology for sensitivity analysis of geometrically nonlinear structures subjected to thermo-mechanical loading in regular and critical states. Thermal post-buckling analysis of uniform, isotropic, slender and shear flexible columns is presented using a rigorous finite element formulation and a much simpler intuitive formulation by Gupta *et al.* (2009). Gupta *et al.* (2010a) investigated simple, elegant, and accurate closed-form expressions for predicting the post-buckling behavior of composite beams with axially immovable ends using the Rayleigh-Ritz method. Thermal post-buckling analysis of columns with axially immovable ends is studied using the Rayleigh-Ritz method by Gupta *et al.* (2010b). Vaz *et al.* (2010) examined elastic buckling and initial post-buckling behavior of slender beams subjected to uniform heating with temperature-dependent physical properties by using a perturbation solution. Akbaş and Kocatürk (2011) investigated post-buckling analysis of a simply supported beam subjected to a uniform thermal loading by using total Lagrangian finite element model of two dimensional continuum for an eight-node quadratic element. Kocatürk and Akbaş (2011) studied post-buckling analysis of

Timoshenko beams with various boundary conditions subjected to a non-uniform thermal loading by using the total Lagrangian Timoshenko beam element approximation. Akbaş (2012) studied termal post-buckling of functionally graded beams. Yu and Sun (2012) investigated large deformation post-buckling of a linear-elastic and hygrothermal beam with axially nonmovable pinned-pinned ends and subjected to a significant increase in swelling by an alternative method. Furthermore, Kocatürk and Akbaş (2012) investigated thermal post-buckling analysis of functionally graded Timoshenko beams subjected to thermal loading by using the total Lagrangian Timoshenko beam element approximation.

It is seen from literature that post-buckling studies with temperature-dependent physical properties has not been broadly investigated. In a recent study, Vaz *et al.* (2010) investigated elastic buckling and initial post-buckling behavior of slender beams subjected to uniform heating taking into account temperature-dependent physical properties by using a perturbation solution. In another recent study, Kocatürk and Akbaş (2011) studied post-buckling analysis of Timoshenko beams with various boundary conditions subjected to a non-uniform thermal loading in the case of temperature independent physical properties by using the total Lagrangian Timoshenko beam element approximation.

Post-buckling behavior of Timoshenko beams subjected to uniform temperature rising with temperature dependent physical properties are studied in this paper by using the total Lagrangian Timoshenko beam element approximation. The considered highly non-linear problem is solved considering full geometric non-linearity by using incremental displacement-based finite element method in conjunction with Newton-Raphson iteration method. The distinctive feature of this study is post-buckling analysis of Timoshenko beams under uniform thermal loading considering full geometric non-linearity and temperature dependent physical properties by using finite element method: As far as the authors know, there is no study on the thermal post-buckling analysis of Timoshenko beams considering full geometric non-linearity and temperature dependent physical properties investigated by using finite element method. Another distinctive feature of this study is investigation of the differences of the analysis results in the case of temperature dependent and independent physical properties in detail in post-buckling case.

The development of the formulations of general solution procedure of nonlinear problems follows the general outline of the derivation given by Zienkiewicz and Taylor (2000). The related formulations of post-buckling analysis of Timoshenko beams with various boundary conditions subjected to a non-uniform thermal loading are obtained by using the total Lagrangian finite element model of Timoshenko beam. Convergence studies are performed for various numbers of elements. In deriving the formulations for post buckling analysis under uniform thermal loading and temperature dependent physical properties, the total Lagrangian Timoshenko beam element formulations given by Felippa (2012) are used. There is no retstriction on the magnitudes of deflections and rotations in contradistinction to von-Karman strain displacement relations of the beam. The difference between temperature dependent and independent physical properties are investigated in detail in post-buckling case. The beams considered in numerical examples are made of Austenitic Stainless Steel (316). The relationships between deflections, thermal post-buckling configuration, critical buckling temperature, maximum stresses of the beams and temperature rising are illustrated in detail in post-buckling case.

2. Theory and formulations

The clamped-clamped beam configurations, with co-ordinate system O (X, Y, Z) are shown in Fig. 1.

In this study, the TL Timoshenko beam element is used and the related formulations are developed for temperature dependent physical properties by using the formulations given by Kocatürk and Akbaş (2011) which was developed for thermal loading by using the formulations given by Felippa (2012). In the present study, finite element model of Timoshenko beam element is developed by using a two-node beam element shown in Fig. 2. Each node has three degrees of freedom: Two node displacements u_{xi} and u_{yi}, and one rotation θ_i about Z axis.

A particle originally located at $P_0(X, Y)$ moves to $P(x, y)$ in the current configuration, as shown in Fig. 3. The projections of P_0 and P along the cross sections at C_0 and C upon the neutral axis are called $C_0(X, 0)$ and $C(x_c, y_c)$, respectively. It will be assumed that dimensions of the beam cross section do not change, and that the shear distortion $\gamma \ll 1$ so that $\cos\gamma$ can be replaced by Felippa (2012)

$$x = x_c - Y(\sin\psi + \sin\gamma\cos\psi) = x_c - Y[\sin(\psi + \gamma) + (1 - \cos\gamma)\sin\psi] = x_c - Y\sin\theta \qquad (1)$$

$$y = y_c + Y(\cos\psi - \sin\gamma\sin\psi) = y_c + Y[\cos(\psi + \gamma) + (1 - \cos\gamma)\cos\psi] = y_c + Y\cos\theta \qquad (2)$$
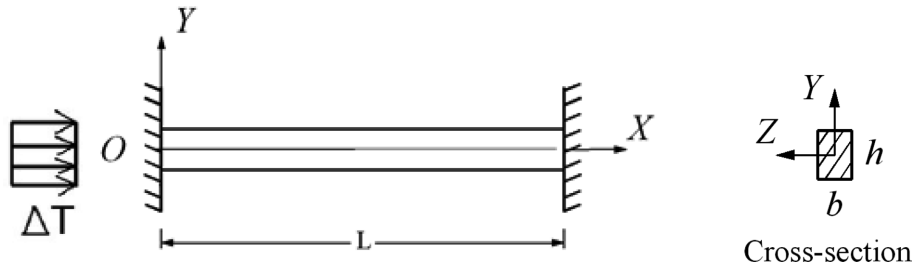

Fig. 1 Clamped-clamped beam subjected to a uniform temperature rise and cross-section
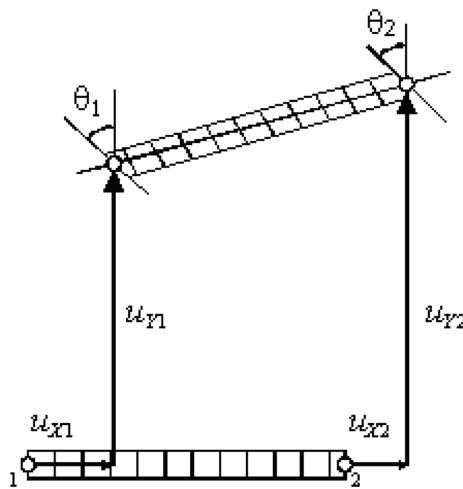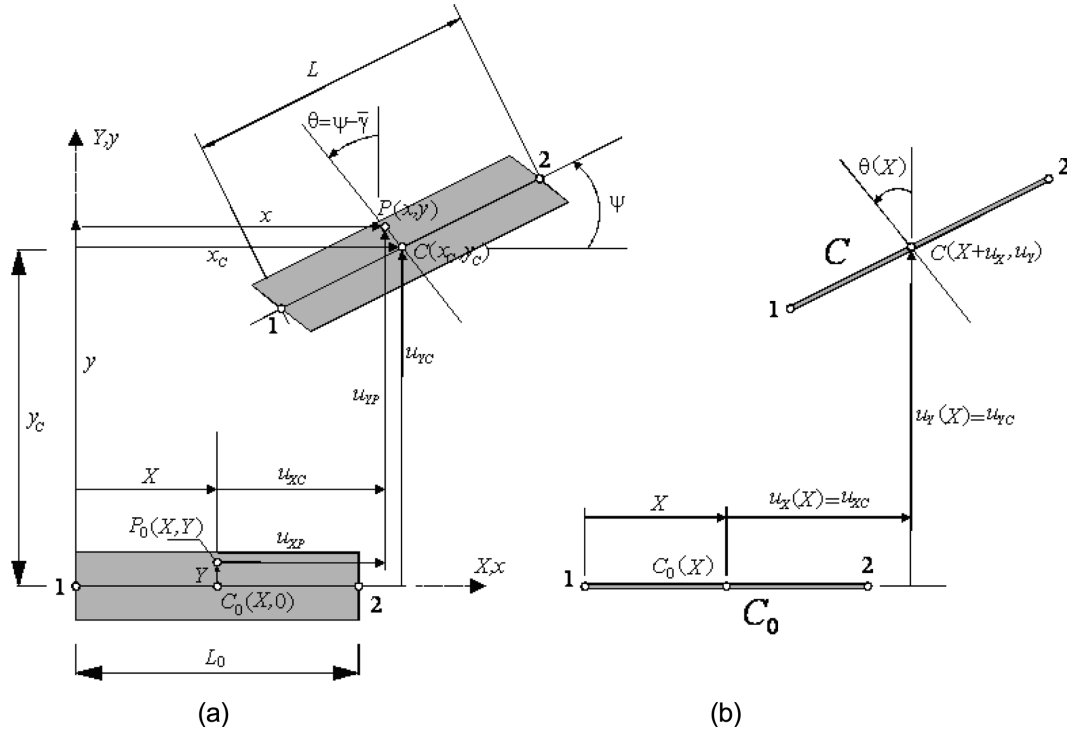

Fig. 2 A two-node C^0 beam element

Fig. 3 Lagrangian kinematics of the C^0 beam element with X-aligned reference configuration: (a) plane beam moving as a two-dimensional body, (b) reduction of motion description to one dimension measured by coordinate X. This figure is given by Felippa (2012)

where $x_c = X + u_{XC}$ and $y_c = u_{XC}$. Consequently, $x = X + u_{XC} - Y\sin\theta$ and $y = u_{YC} + Y\cos\theta$. From now on we shall call u_{XC} and u_{YC} simply u_X and u_Y, respectively, so that the Lagrangian representation of the motion is

$$\begin{bmatrix} X \\ Y \end{bmatrix} = \begin{bmatrix} X + u_X - Y\sin\theta \\ u_Y + Y\cos\theta \end{bmatrix} \tag{3}$$

in which u_X, u_Y and θ are functions of X only. This concludes the reduction to a one-dimensional model, as sketched in Fig. 3(b). For a two-node C_0 element, it is natural to express the displacements and rotation functions as linear in between the node displacements

$$\mathbf{w} = \begin{bmatrix} u_X(X) \\ u_Y(X) \\ \theta(X) \end{bmatrix} = \frac{1}{2}\begin{bmatrix} 1-\xi & 0 & 0 & 1+\xi & 0 & 0 \\ 0 & 1-\xi & 0 & 0 & 1+\xi & 0 \\ 0 & 0 & 1-\xi & 0 & 0 & 1+\xi \end{bmatrix}\begin{bmatrix} u_{X1} \\ u_{Y1} \\ \theta_1 \\ u_{X2} \\ u_{Y2} \\ \theta_2 \end{bmatrix} = \mathbf{Nu} \tag{4}$$

in which $\xi = (2X/L_0) - 1$ is the isoparametric coordinate that varies from $\xi = -1$ at node 1 to $\xi = 1$ at node 2.

The Green-Lagrange strains are given as follows Felippa (2012)

$$[\mathbf{e}] = \begin{bmatrix} e_1 \\ e_2 \end{bmatrix} = \begin{bmatrix} e_{XX} \\ 2e_{XY} \end{bmatrix} = \begin{bmatrix} (1+u_X')\cos\theta + u_Y'\sin\theta - Y\theta' - 1 \\ -(1+u_X')\sin\theta + u_Y'\sin\theta \end{bmatrix} = \begin{bmatrix} e - Y\kappa \\ \gamma \end{bmatrix} \tag{5}$$

$$e = (1+u_X')\cos\theta + u_Y'\sin\theta - 1 \; ; \quad \gamma = -(1+u_X')\sin\theta + u_Y'\sin\theta; \quad \kappa = \theta' \tag{6}$$

where e is the axial strain, γ is the shear strain and κ is curvature of the beam, $u_X' = du_X/dX$, $u_Y' = du_Y/dX$, $\theta' = d\theta/dX$. The second Piola-Kirchhoff stresses with a temperature rise can be expressed by inclusion of the temperature term as follows

$$\mathbf{s} = \begin{bmatrix} s_{XX} \\ s_{XY} \end{bmatrix} = \begin{bmatrix} s_1 \\ s_2 \end{bmatrix} = \begin{bmatrix} s_1^0 + E(T)(e_1 - \alpha_X(T)\Delta T) \\ s_2^0 + G(T)e_2 \end{bmatrix} = \begin{bmatrix} s_1^0 \\ s_2^0 \end{bmatrix} + \begin{bmatrix} E(T) & 0 \\ 0 & G(T) \end{bmatrix} \begin{bmatrix} e_1 - \alpha_X(T)\Delta T \\ e_2 \end{bmatrix} \tag{7}$$

where s_1^0, s_2^0 are initial stresses, E is Young's modulus and G is the shear modulus, α_X is coefficient of thermal expansion in the X direction and $T = T_0 + \Delta T$, where T_0 is installation temperature and ΔT is the uniform temperature rise. The physical properties of the material (Young's modulus, coefficient of thermal expansion, yield stress) are dependent on temperature T.

The beams considered in numerical examples are made of Austenitic Stainless Steel (316). The coefficients of temperature T for Austenitic Stainless Steel (316) are expressed as follows (from Incropera and DeWitt 1985, Detail of the ITER Outline Design Report 1994, ITER Documentation Series: No 29 1991, ASME Code Cases: Nuclear Components 1992)

$$E(T) = 205.91 - 2.6913 \times 10^{-2}\, T - 4.1876 \times 10^{-5}\, T^2 \text{ (GPa)} \tag{8}$$

$$\alpha(T) = (11.813 + 1.3106 \times 10^{-2}\, T - 6.1375 \times 10^{-6}\, T) \times 10^{-6} \text{ (m/mK)} \tag{9}$$

$$\sigma_y(T) = 448.69 - 1.193\,T + 1.4787 \times 10^{-3}\, T^2 - 6.3134 \times 10^{-7}\, T^3 \text{ (MPa)} \tag{10}$$

where E is Young's modulus, α_X is thermal expansion coefficient and σ_y is yield stress. Poisson's ratio is taken as $\nu = 0.27$. In this study, the unit of the temperature is taken as Kelvin (K). These equations are valid for temperatures ranging from 300 K to 1000 K.

Using constitutive Eq. (7), axial force N, shear force V and bending moment M can be obtained as

$$N = \int_A s_1 dA = \int_A [s_1^0 + E(T)(e - Y\kappa - \alpha_X(T)\Delta T)]dA \tag{11}$$

$$N = N^0 + E(T)eA - E(T)A\,\alpha_X(T)\Delta T \tag{12}$$

$$V = \int_A s_2 dA = \int_A [s_2^0 + G(T)e_2]dA = V^0 + G(T)A\gamma \tag{13}$$

$$M = \int_A -Y s_1 dA = \int_A -Y[s_1^0 + E(T)(e - Y\kappa - \alpha_X(T)\Delta T)]dA \tag{14}$$

$$M = M^0 + EI_0\kappa \tag{15}$$

where A and I_0 are the cross section area and second moment of inertia, respectively.

$$N^0 = \int_{A_0} s_1^0 dA, \quad V^0 = \int_{A_0} s_2^0 dA, \quad M^0 = \int_{A_0} -Ys_1^0 dA \tag{16}$$

For the solution of the total Lagrangian formulations of TL Timoshenko beam problem, small-step incremental approaches from known solutions are used. As it is known, it is possible to obtain solutions in a single increment of the external force only in the case of mild nonlinearity (and no path dependence). To obtain realistic answers, physical insight into the nature of the problem and, usually, small-step incremental approaches from known solutions are essential. Such increments are always required if the constitutive law relating stress and strain changes is path dependent. Also, such incremental procedures are useful to reduce excessive numbers of iterations and in following the physically correct path. In the iterations, the temperature loading is divided by a suitable number according to the value of temperature. In high temperature values, the temperature loading is divided by large numbers. After completing an iteration process, the load is increased by adding load increment to the accumulated load.

In this study, small-step incremental approaches from known solutions with Newton-Raphson iteration method are used in which the solution for $n+1$th load increment and ith iteration is obtained in the following form

$$d\mathbf{u}_n^i = (\mathbf{K}_T^i)^{-1}\mathbf{R}_{n+1}^i \tag{17}$$

where $(K_T^i)_S$ is the system stiffness matrix corresponding to a tangent direction at the ith iteration, $d\mathbf{u}_n^i$ is the solution increment vector at the ith iteration and $n+1$th load increment, $(R_{n+1}^i)_S$ is the system residual vector at the ith iteration and $n+1$th load increment. This iteration procedure is continued until the difference between two successive solution vectors is less than a selected tolerance criterion in Euclidean norm given by

$$\sqrt{\frac{(d\mathbf{u}_n^{i+1} - d\mathbf{u}_n^i)^T(d\mathbf{u}_n^{i+1} - d\mathbf{u}_n^i)^2}{[(d\mathbf{u}_n^{i+1})^T(d\mathbf{u}_n^{i+1})^2]}} \leq \zeta_{tol} \tag{18}$$

A series of successive approximations gives

$$\mathbf{u}_{n+1}^{i+1} = \mathbf{u}_{n+1}^i + d\mathbf{u}_{n+1}^i = \mathbf{u}_n + \Delta\mathbf{u}_n^i \tag{19}$$

where

$$\Delta\mathbf{u}_n^i = \sum_{k=1}^{i} d\mathbf{u}_n^k \tag{20}$$

The residual vector $\mathbf{R}_{n+1}^i$ for a finite element is as follows

$$\mathbf{R}_{n+1}^i = \mathbf{f} - \mathbf{p} \tag{21}$$

where $\mathbf{f}$ is the vector of external forces and $\mathbf{p}$ is the vector of internal forces given in Appendix.

The element tangent stiffness matrix for the total Lagrangian Timoshenko plane beam element is as follows which is given by Kocatürk and Akbaş (2011), Felippa (2012)

$$\mathbf{K}_T = \mathbf{K}_M + \mathbf{K}_G \tag{22}$$

where $\mathbf{K}_G$ is the geometric stiffness matrix, and $\mathbf{K}_M$ is the material stiffness matrix given as follows by Kocatürk and Akbaş (2011), Felippa (2012)

$$\mathbf{K}_M = \int_{L_0} \mathbf{B}_m^T \mathbf{S} \mathbf{B}_m dX \tag{23}$$

The explicit forms of the expressions in Eq. (22) is given in Appendix. After integration of Eq. (23), K_M can be expressed as follows

$$\mathbf{K}_M = \mathbf{K}_M^a + \mathbf{K}_M^b + \mathbf{K}_M^s \tag{24}$$

where $\mathbf{K}_M^a$ is the axial stiffness matrix, $\mathbf{K}_M^b$ is the bending stiffness matrix, $\mathbf{K}_M^s$ is the shearing stiffness matrix and explicit forms of these expressions remain the same as given by Kocatürk and Akbaş (2011) except for modulus of elasticity E depends on temperature T in the present study. The details of these expressions are given in Appendix.

The geometric stiffness matrix K_G, $\mathbf{B}_m$ and the internal nodal force vector $\mathbf{p}$ remains the same as given by Kocatürk and Akbaş (2011), Felippa (2012) and given in Appendix.

After obtaining the displacements of nodes, the second Piola-Kirchhoff stress tensor components S_{xx}, S_{xy}, S_{yy} can be obtained by using Eq. (7). The relation between the Cauchy stress tensor components $\sigma_{xx}, \sigma_{xy}, \sigma_{yy}$ and the second Piola-Kirchhoff stress tensor components S_{xx}, S_{xy}, S_{yy} is given in Kocatürk and Akbaş (2011).

The beams considered in numerical examples are elastic, with undeformed length L, rectangular cross-section of width b and thickness h (see Fig. 1).

3. Numerical results

In the numerical examples, the post-buckling deflections as well as the max. Cauchy normal stresses, thermal post-buckling configuration, critical buckling temperatures are calculated and presented in figures for temperature dependent and independent physical properties for various thermal loads. To this end, by use of usual assembly process, the system tangent stiffness matrix and the system residual vector are obtained by using the element stiffness matrixes and element residual vectors for the total Lagrangian Timoshenko plane beam element. After that, the solution process outlined in the previous section is used for obtaining the related solutions for the total Lagrangian finite element model of Timoshenko plane beam element.

The beams considered in numerical examples are made of Austenitic Stainless Steel (316). The coefficients of temperature T for Austenitic Stainless Steel (316) are expressed as follows (from Incropera and DeWitt 1985, Detail of the ITER Outline Design Report 1994, ITER Documentation Series: No 29 1991, ASME Code Cases: Nuclear Components 1992). In this study, the material of the beam is considered in the elastic range, so as not to exceed the yield stress (σ_y) that is a

Table 1 Convergence analysis for the central deflections $V(L/2)$ of the beam
for various numbers of finite elements n for $\Delta T = 35$ K and $L/h = 80$

The central deflections $V(L/2)$ of the beam	
n	$V(L/2)$ (m)
20	0.2349
30	0.2596
40	0.2676
50	0.2712
60	0.2732
70	0.2744
80	0.2750
90	0.2754
100	0.2756
110	0.2757
120	0.2757

function of temperature. Hence, if the stress of the beam equals to yield stress, then the analysis is interrupted. So, plastic buckling and plastic post-buckling cases are not considered in this study.

In numerical examples, the initial temperature (installation temperature) of the beam is assumed to be $T_0 = 300$ K. The height of the beam is $h = 1$ m and the width of the beam is $b = 1$ m. Convergence studies are also performed. In the post-buckling case, the maximum Cauchy stresses (true stresses) can be obtained after obtaining the second Piola-Kirchhoff stresses by using the relations between the Cauchy and the second Piola-Kirchhoff stresses tensor components given by Kocatürk and Akbaş (2011), Felippa (2012).

In Table 1, the central deflections $V(L/2)$ of the beam for uniform temperature rise $\Delta T = 35$ K are calculated for various numbers of finite elements n for $L/h = 80$, $b = 1$ m, $h = 1$ m with temperature-dependent physical properties. Where, temperature rise $\Delta T = 35$ K corresponds to yield temperature for $L/h = 80$ in the post-buckling case which is plotted in Fig. 8.

It is seen from Table 1 that, when the number of finite elements is $n = 120$, the considered displacements converge. Therefore, in the numerical calculations, the number of finite elements is taken as $n = 120$.

Young's Modulus and the coefficient of thermal expansion versus temperature rising are illustrated in Fig. 4 and yield stress versus temperature rising are illustrated in Fig. 5, by using Eqs. (9), (10) and (11) respectively for Austenitic Stainless Steel (316).

It is seen from Fig. 4 that with increase in temperature, Young's modulus decreases. Because, with the temperature increase, the intermolecular distances of the material increase and intermolecular forces decrease. As a result, the strength of the material decreases. Also, It is seen from Fig. 4 that, with temperature increase, the coefficient of thermal expansion increases. It is seen from Fig. 5 that, increase in temperature causes decrease in the yield stresses.

In Fig. 6, thermal post-buckling configuration of the beam is presented for $L/h = 100$, $b = 1$ m, $h = 1$ m for uniform temperature rising $\Delta T = 25$ K and also for elastic post-buckling temperature limits for temperature dependent and independent physical properties.
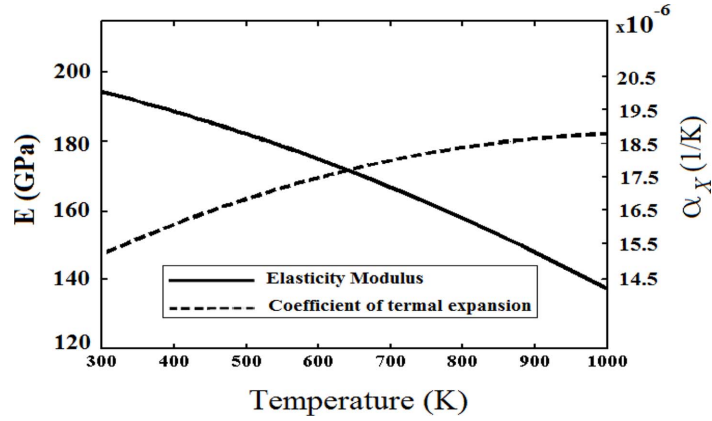
Fig. 4 Young's modulus and coefficient of thermal expansion of Austenitic Stainless Steel (316) versus temperature rising
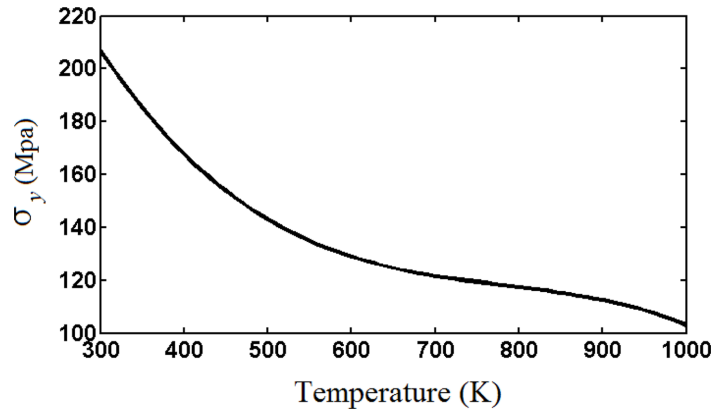

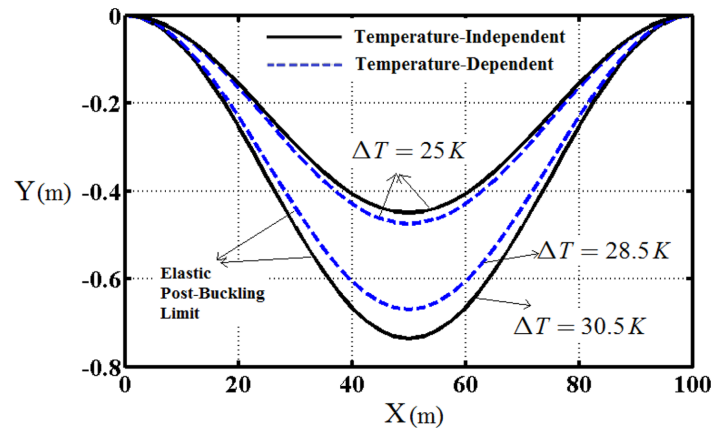Fig. 5 Yield stress of Austenitic Stainless Steel (316) versus temperature rising

Fig. 6 Thermal Post-Buckling configuration of the beam for $L/h = 100$, $b = 1$ m, $h = 1$ m for uniform temperature rising $\Delta T = 25$ K and elastic post-buckling temperature limit with temperature dependent and independent physical properties
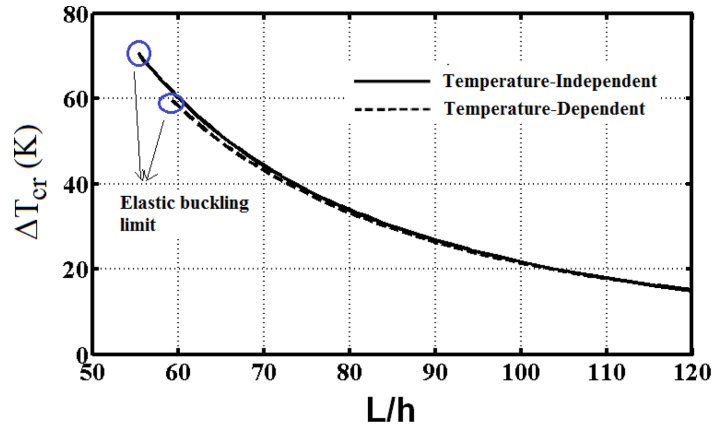
Fig. 7 Critical buckling uniform temperature ΔT versus the ratio L/h with temperature dependent and independent physical properties

It is seen from Fig. 6 that, there is a significant difference between the deformed configurations of the beam for temperature dependent and temperature independent physical properties. Also it is seen from Fig. 6 that the elastic limit for temperature dependent physical properties are lower than the elastic limit for temperature independent physical properties: Because, with temperature rising, the yield stress of the material decrease.

In Fig. 7, the critical buckling uniform temperature ΔT versus the ratio L/h of the beam is presented for temperature dependent and independent physical properties for $b = 1$ m and $h = 1$ m.

It seen from Fig. 7 that, the beam buckles at lower temperatures for higher L/h ratios. Decrease of the ratio L/h of the beam causes increase in the difference between the critical buckling temperatures for the temperature dependent and independent physical properties. Approximately after $L/h = 70$, the critical buckling temperatures of the temperature dependent and independent physical properties almost coincide. In small L/h ratios, the critical temperatures for the temperature-independent physical properties are greater than the critical temperatures of the temperature-dependent physical properties. Also elastic buckling limit of the beam with temperature independent physical properties is obtained at a lower L/h ratio compared to the elastic buckling limit of the beam with temperature dependent properties. Hence, the temperature-dependent physical properties must be taken into account for safe design of beams and for obtaining more realistic results. Otherwise an important error is inevitable.

In Fig. 8, the specified transversal displacement $v(L/2)$ versus uniform temperature rising ΔT is presented for temperature dependent and independent physical properties for $L/h = 80$, 90, 100 ratios.

It is seen from Fig. 8 that the difference of the transversal displacements of the midpoint of the beam with the temperature dependent and independent physical properties in post-buckling case increases with decrease in the ratio L/h. In other words, increase in the ratio L/h of the beam causes decrease in the difference between the transversal displacements for the temperature dependent and independent physical properties. In Fig. 8, furcation points can be seen. As it is known, buckling occurs at the furcation points: Actually these points are bifurcation points. As it is konown, according to the initial arbitrary deviation from the straight position of the beam, buckling can occur in either positive or negative directions. In this study, deviation from the straight position is always

taken as positive for buckling analysis. The symmetrical branches according to ΔT axis would be obtained if the deviations from the straight positions were taken as negative values. The transversal displacements for the temperature-dependent physical properties are greater than those for the temperature-independent physical properties. This situation may be explained as follows: In the temperature-dependent physical properties, with the temperature increase, the intermolecular distances of the material increase and intermolecular forces decrease. As a result, the strength of the material decreases. Hence, the beam becomes more flexible in the case of the temperature-dependent physical properties.

Also, it is seen from Fig. 8 that the material of the beam yields after certain temperatures that are shown by circles on the figures in the post-buckling case: After the corresponding temperature, plasticity must be considered which is out of the scope of this study.
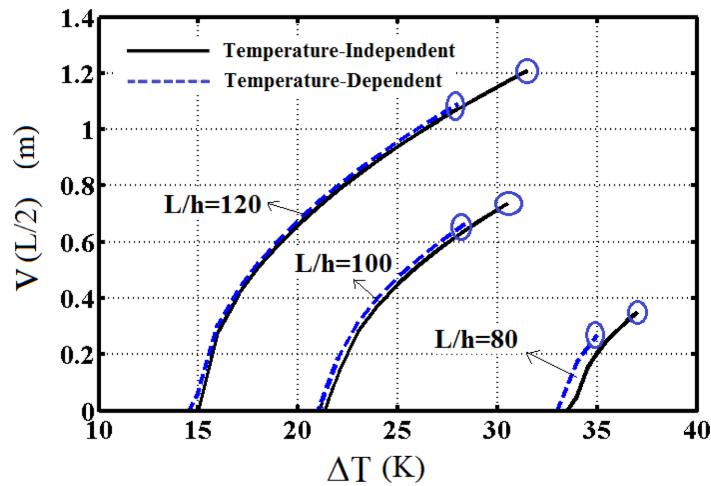
Fig. 8 The specified transversal displacment $v(L/2)$ versus uniform temperature rising ΔT with temperature dependent and independent physical properties for the ratio $L/h = 80, 90, 100$
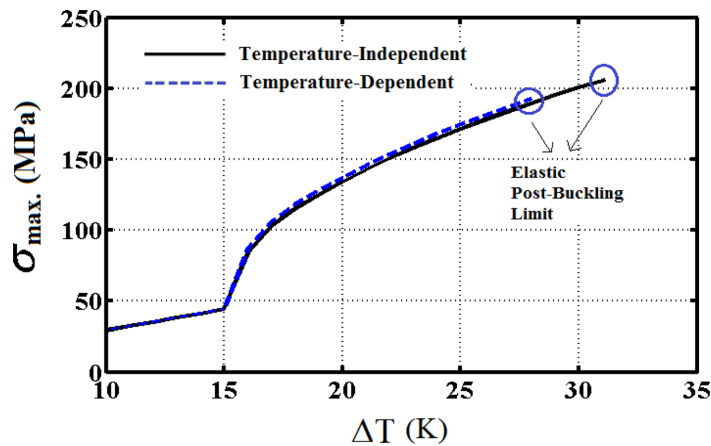
Fig. 9 Maximum Cauchy normal stress versus uniform temperature rising ΔT for temperature dependent and independent physical properties for $L/h = 120$, $b = 1$ m and $h = 1$ m

In Fig. 9, maximum Cauchy normal stresses versus uniform temperature rising ΔT is presented for temperature dependent and independent physical properties for $L/h = 120$, $b = 1$ m and $h = 1$ m.

The maximum Cauchy normal stresses for the temperature dependent and independent physical properties in the post-buckling case within elastic limit are given in Fig. 9. Before the buckling furcation point, the maximum Cauchy normal stresses increase almost linearly, but after furcation point, the stresses increase suddenly. This situation is expected and natural in buckling phenomenon. Also, it is seen from Fig. 9 that the yield stress for the beam with temperature dependent physical properties is lower than the yield stress for the beam with temperature independent physical properties.

4. Conclusions

Thermal post-buckling analysis of a Timoshenko beam subjected to uniform temperature rising is investigated for temperature dependent physical properties by using the total Lagrangian Timoshenko beam element approximation. The considered highly non-linear problem is solved considering full geometric non-linearity by using incremental displacement-based finite element method in conjunction with Newton-Raphson iteration method. The difference between the analysis results for the temperature dependent and independent physical properties are investigated in detail in post-buckling case. The relationships between deflections, thermal post-buckling configurations, critical buckling temperatures, maximum stresses of the beams and temperature rising are illustrated in detail in post-buckling case. It is observed from the investigations that there are significant differences of the analysis results for the temperature dependent and independent physical properties in the post-buckling case. Especially, increase in temperature causes increase in the difference of the analysis results for the temperature dependent and independent physical properties considerably. After certain temperatures, the material of the beam yields. The yield stresses of material for temperature dependent physical properties are lower than the yield stresses of temperature independent physical properties. Hence, for safe design of structural elements, the temperature-dependent physical properties must be considered. Otherwise an important error is inevitable. Also, increase of the ratio L/h of the beam causes decrease in the difference between the transversal displacements for the temperature dependent and independent physical properties. It is observed from open literature that the effect of temperature dependent physical properties on the analysis results are not considered broadly. Taking into consideration of the temperature dependent physical properties is very important for failure analysis and safe design of structures.

References

Akbaş, Ş.D. (2012), "Post-buckling behaviour of functionally graded beams under the influence of temperature", Ph.D. Thesis, Institute of Science at Yıldız Technical University Istanbul.

Akbaş, Ş.D. and Kocatürk, T. (2011), "Post-buckling analysis of a simply supported beam under uniform thermal loading", *Sci. Res. Essays,* **6**(4), 1135-1142.

Aristizabal-Ochoa, J.D. (2007), "Large deflection and post-buckling behavior of Timoshenko beam-columns with semi-rigid connections including shear and axial effects", *J. Eng. Struct.,* **29**(6), 991-1003.

ASME Code Cases : Nuclear Components (1992), Case N-47-30, Section III, Division 1, ASME Boiler and Pressure Vessel Code.

Chen, B., Gu, Y., Zhao, G., Lin, W., Chang T.Y.P. and Kuang, J.S. (2003), "Design optimization for structural

thermal buckling", *J. Therm. Stresses*, **26**(5), 479-494.

Coffin, D.W. and Bloom, F. (1999), "Elastica solution for the hygrothermal buckling of a beam", *Int. J. Nonlin. Mech.,* **34**(5), 935-947.

Detail of the ITER Outline Design Report (1994), The ITER Machine, Vol 2, San Diego.

Parente, E. and de Sousa, J.M.S. (2008), "Design sensitivity analysis of nonlinear structures subjected to thermal loads", *Comput. Struct.,* **86**(11-12), 1369-1384.

Felippa, C.A., Retrieved March (2012), "Notes on nonlinear finite element methods", http://www.colorado.edu/engineering/cas/courses.d/NFEM.d/NFEM.Ch10.d/NFEM.Ch10.pdf

Gauss, R.C. and Antman, S.S. (1984), "Large thermal buckling of non-uniform beam and plates", *Int. J. Solids Struct.*, **20**(11-12), 979-1000.

Gupta, R.K., Gunda, J.B., Janardhan, G.R. and Rao, G.V. (2009), "Comparative study of thermal post-buckling analysis of uniform slender & shear flexible columns using rigorous finite element and intutive formulations", *Int. J. Mech. Sci.,* **51**(3), 204-212.

Gupta, R.K., Gunda, J.B., Janardhan, G.R. and Rao, G.V. (2010a), "Post-buckling analysis of composite beams: Simple and accurate closed-form expressions", *Compos. Struct.,* **92**(3)*,* 1947-1956.

Gupta, R.K., Gunda, J.B., Janardhan, G.R. and Rao, G.V. (2010b), "Thermal post-buckling analysis of slender columns using the concept of coupled displacement field", *Int. J. Mech. Sci.,* **52**(4)*,* 590-594.

Incropera, F. and DeWitt, D. (1985), *Fundamentals of Heat and Mass Transfer*, 2nd Edition, John Wiley.

ITER Documentation Series, No 29 (1991), Blanket, Shield Design and Material Data Base, IAEA, Vienna.

Jekot, T. (1996), "Non-linear problems of thermal buckling of a beam", *J. Therm. Stresses*, **19**, 359-369.

Kocatürk, T. and Akbaş, Ş.D. (2011), "Post-buckling analysis of Timoshenko beams with various boundary conditions under non-uniform thermal loading", *Struct. Eng. Mech.*, **40**(3), 347-371.

Kocatürk, T. and Akbaş, Ş.D. (2012), "Post-buckling analysis of Timoshenko beams made of functionally graded material under thermal loading", *Struct. Eng. Mech.*, **41**(6), 775-789.

Li, S.R. (2000), "Thermal post-buckling of asymmetrically supported elastic rods", *Eng. Mech.,* **17**(5), 115-119.

Li, S. and Cheng, C. (2000), "Analysis of thermal post- buckling of heated elastic rods", *Appl. Math. Mech. (English Ed.)*, **21**(2), 133-140.

Li, S., Zhou, Y.H. and Zheng, X. (2002), "Thermal post- buckling of a heated elastic rod with pinned-fixed ends", *J. Therm. Stresses*, **25**(1), 45-56.

Li, S. and Zhou, Y. (2001), "Thermal post-buckling of rods with variable cross sections", *Proceedings of the Fourth International Congress on Thermal Stresses*, Osaka, Japan.

Li, S.R., Cheng, C.J. and Zhou, Y.H. (2003), "Thermal post-buckling of an elastic beams subjected to a transversely non-uniform temperature rising", *Appl. Math. Mech. (English Ed.)*, **24**(5), 514-520.

Li, S. and Zhou, Y. (2003), "Geometrically nonlinear analysis of Timoshenko beams under thermomechanical loadings", *J. Therm. Stresses*, **26**(9), 861-872.

Li, S. and Song, X. (2006), "Large thermal deflections of Timoshenko beams under transversely non-uniform temperature rise", *Mech. Res. Commun.*, **33**(1), 84-92.

Rao, G.V. and Raju, K.K. (1984), "Thermal postbuckling of columns", *AIAA J.*, **22**(6), 850-851.

Song, X. and Li, S.R. (2007), "Thermal buckling and post-buckling of pinned-fixed Euler-Bernoulli beams on an elastic foundation", *Mech. Res. Commun.*, **34**(2), 164-171.

Vaz, M.A. and Solano, R.F. (2003), "Postbuckling analysis of slender elastic rods subjected to uniform thermal loads", *J. Therm. Stresses*, **26**(9), 847-860.

Vaz, M.A. and Solano, R.F. (2004), "Thermal post-buckling of slender elastic rods with hinged ends constrained by a linear spring", *J. Therm. Stresses,* **27**(4), 367-380.

Vaz, M.A., Nascimento, M.S. and Solano, R.F. (2007), "Initial post-buckling of elastic rods subjected to thermal loads and resting on an elastic foundation", *J. Therm. Stresses,* **30**(4), 381-393.

Vaz, M.A., Cyrino, J.C.R. and Neves, A.C. (2010), "Initial thermo-mechanicalpost-buckling of beams with temperature-dependent physical properties", *Int. J. Nonlin. Mech.,* **45**(3), 256-262.

Yu, Y.P. and Sun, Y.H. (2012), "Analytical approximate solutions for large post-buckling response of a hygrothermal beam", *Struct. Eng. Mech.*, **43**(2), 211-223.

Zienkiewicz, O.C. and Taylor, R.L. (2000), *The Finite Element Method*, Fifth Edition, Volume 2: Solid Mechanics, Butterworth-Heinemann, Oxford.

Appendix

The components of the material stiffness matrix: the axial stiffness matrix $\mathbf{K}_M^a$, bending stiffness matrix $\mathbf{K}_M^b$ and shearing stiffness matrix $\mathbf{K}_M^s$ are as follows

$$
\mathbf{K}_M^a = \frac{E(T)A_0}{L_0}
\begin{bmatrix}
c_m^2 & c_m s_m & -c_m\gamma_m L_0/2 & -c_m^2 & -c_m s_m & -c_m\gamma_m L_0/2 \\
c_m s_m & s_m^2 & -\gamma_m L_0 s_m/2 & -c_m s_m & -s_m^2 & -\gamma_m L_0 s_m/2 \\
-c_m\gamma_m L_0/2 & -\gamma_m L_0 s_m/2 & \gamma_m^2 L_0^2/4 & c_m\gamma_m L_0/2 & \gamma_m L_0 s_m/2 & \gamma_m^2 L_0^2/4 \\
-c_m^2 & -c_m s_m & c_m\gamma_m L_0/2 & c_m^2 & c_m s_m & c_m\gamma_m L_0/2 \\
-c_m s_m & -s_m^2 & \gamma_m L_0 s_m/2 & c_m s_m & s_m^2 & \gamma_m L_0 s_m/2 \\
-c_m\gamma_m L_0/2 & -\gamma_m L_0 s_m/2 & \gamma_m^2 L_0^2/4 & c_m\gamma_m L_0/2 & \gamma_m L_0 s_m/2 & \gamma_m^2 L_0^2/4
\end{bmatrix}
\tag{A1}
$$

$$
\mathbf{K}_M^b = \frac{E(T)I_0}{L_0}
\begin{bmatrix}
0 & 0 & 0 & 0 & 0 & 0 \\
0 & 0 & 0 & 0 & 0 & 0 \\
0 & 0 & 1 & 0 & 0 & -1 \\
0 & 0 & 0 & 0 & 0 & 0 \\
0 & 0 & 0 & 0 & 0 & 0 \\
0 & 0 & -1 & 0 & 0 & 1
\end{bmatrix}
\tag{A2}
$$

$$
\mathbf{K}_M^s = \frac{G(T)A_0}{L_0}
\begin{bmatrix}
s_m^2 & -c_m s_m & -\alpha_1 L_0 s_m/2 & -s_m^2 & c_m s_m & -\alpha_1 L_0 s_m/2 \\
-c_m s_m & c_m^2 & c_m\alpha_1 L_0/2 & c_m s_m & -c_m^2 & c_m\alpha_1 L_0/2 \\
-\alpha_1 L_0 s_m/2 & c_m\alpha_1 L_0/2 & \alpha_1^2 L_0^2/4 & \alpha_1 L_0 s_m/2 & -c_m\alpha_1 L_0/2 & \alpha_1^2 L_0^2/4 \\
-s_m^2 & c_m s_m & \alpha_1 L_0 s_m/2 & s_m^2 & -c_m s_m & \alpha_1 L_0 s_m/2 \\
c_m s_m & -c_m^2 & -c_m\alpha_1 L_0/2 & -c_m s_m & c_m^2 & -c_m\alpha_1 L_0/2 \\
-\alpha_1 L_0 s_m/2 & c_m\alpha_1 L_0/2 & \alpha_1^2 L_0^2/4 & \alpha_1 L_0 s_m/2 & -c_m\alpha_1 L_0/2 & \alpha_1^2 L_0^2/4
\end{bmatrix}
\tag{A3}
$$

where m stands for beam midpoint, $\xi = 0$, and $\theta_m = (\theta_1 + \theta_1)/2$, $\omega_m = \theta_m + \varphi$, $c_m = \cos\omega_m$, $s_m = \sin\omega_m$, $e_m = L\cos(\theta_m - \psi)/L_0 - 1$, $\alpha_1 = 1 + e_m$ and $\gamma_m = L\sin(\psi - \theta_m)/L_0$ (See Fig. A1 for symbols). The axis of the considered beam initially is taken as horizontal, therefore $\varphi = 0$. The matrix $\mathbf{S}$ is defined as follows

$$
\mathbf{S} =
\begin{bmatrix}
E(T)A_0 & 0 & 0 \\
0 & G(T)A_0 & 0 \\
0 & 0 & I_0 A_0
\end{bmatrix}
\tag{A4}
$$

$\mathbf{B}_m$ matrix is as follows

$$
\mathbf{B}_m = \mathbf{B}\big|_{\xi=0} = \frac{1}{L_0}
\begin{bmatrix}
-c_m & -s_m & -\dfrac{1}{2}L_0\gamma_m & c_m & s_m & -\dfrac{1}{2}L_0\gamma_m \\
s_m & -c_m & \dfrac{1}{2}L_0(1+e_m) & s_m & -c_m & \dfrac{1}{2}L_0(1+e_m) \\
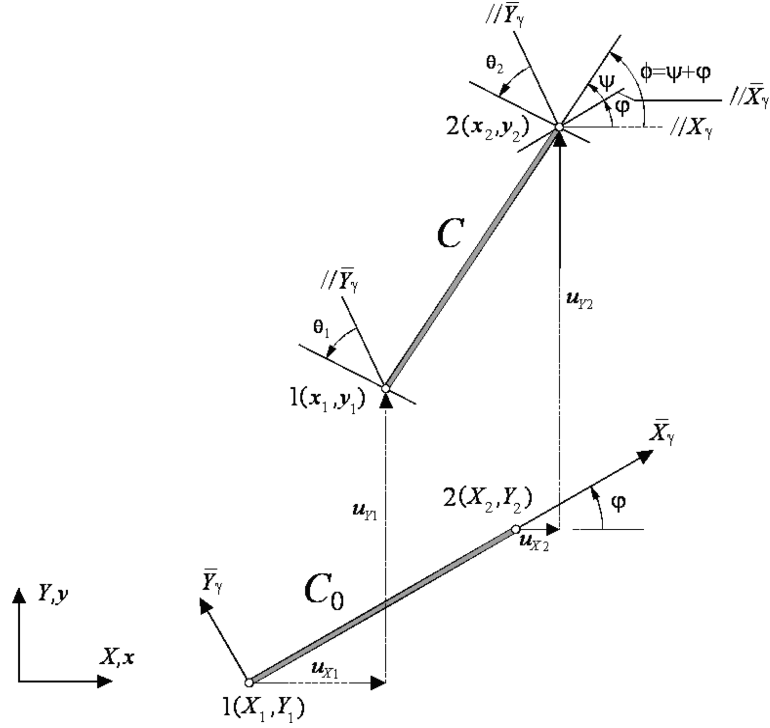0 & 0 & -1 & 0 & 0 & 1
\end{bmatrix}
\tag{A5}
$$

Fig. A1 Plane beam element with arbitrarily oriented reference configuration (Felippa 2012)

The geometric stiffness matrix K_G is given as follows

$$
\mathbf{K}_G = \frac{N_m}{2} \begin{bmatrix}
0 & 0 & s_m & 0 & 0 & s_m \\
0 & 0 & -c_m & 0 & 0 & -c_m \\
s_m & -c_m & -\frac{1}{2}L_0(1+e_m) & -s_m & c_m & -\frac{1}{2}L_0(1+e_m) \\
0 & 0 & -s_m & 0 & 0 & -s_m \\
0 & 0 & c_m & 0 & 0 & c_m \\
s_m & -c_m & -\frac{1}{2}L_0(1+e_m) & -s_m & c_m & -\frac{1}{2}L_0(1+e_m)
\end{bmatrix}
$$

$$
+ \frac{V_m}{2} \begin{bmatrix}
0 & 0 & c_m & 0 & 0 & c_m \\
0 & 0 & s_m & 0 & 0 & s_m \\
c_m & s_m & -\frac{1}{2}L_0\gamma_m & -c_m & -s_m & -\frac{1}{2}L_0\gamma_m \\
0 & 0 & -c_m & 0 & 0 & -c_m \\
0 & 0 & -s_m & 0 & 0 & -s_m \\
c_m & s_m & -\frac{1}{2}L_0\gamma_m & -c_m & -s_m & -\frac{1}{2}L_0\gamma_m
\end{bmatrix} \tag{A6}
$$

in which N_m and V_m are the axial and shear forces which are evaluated at the midpoint. The internal nodal force vector is as follows Felippa (2012)

$$\mathbf{p} = L_0 \mathbf{B}_m^T \mathbf{z} = \begin{bmatrix} -c_m & -s_m & \frac{1}{2}L_0\gamma_m & c_m & s_m & \frac{1}{2}L_0\gamma_m \\ s_m & -c_m & -\frac{1}{2}L_0(1+e_m) & s_m & -c_m & -\frac{1}{2}L_0(1+e_m) \\ 0 & 0 & -1 & 0 & 0 & 1 \end{bmatrix}^T \begin{bmatrix} N \\ V \\ M \end{bmatrix} \tag{A7}$$

where $\mathbf{z}^T = [N\ V\ M]$. The external nodal force vector can be expressed as follows

$$\mathbf{f} = h_e \int_h \int_{L_0} \begin{bmatrix} 1-\xi_1 & 0 & 0 \\ 0 & 1-\xi_1 & 0 \\ 0 & 0 & 1-\xi_1 \\ 1-\xi_2 & 0 & 0 \\ 0 & 1-\xi_2 & 0 \\ 0 & 0 & 1-\xi_2 \end{bmatrix} \begin{bmatrix} f_X \\ f_Y \\ 0 \end{bmatrix} dXdY + b\int_{L_0} \begin{bmatrix} 1-\xi_1 & 0 & 0 \\ 0 & 1-\xi_1 & 0 \\ 0 & 0 & 1-\xi_1 \\ 1-\xi_2 & 0 & 0 \\ 0 & 1-\xi_2 & 0 \\ 0 & 0 & 1-\xi_2 \end{bmatrix} \begin{bmatrix} t_x \\ t_Y \\ m_Z \end{bmatrix} dX \tag{A8}$$

where f_X, f_Y are the body forces, t_X, t_Y, m_Z are the surface loads in the X, Y directions and about the Z axis, h_e is the thickness, h is the height.